Acta Crystallographica Section F
Structural Biology and Crystallization Communications
ISSN 1744-3091

Crystallization and preliminary X-ray characterization of the nitrile reductase QueF: a queuosine-biosynthesis enzyme

Manal A. Swairjo,[a]* Robert R. Reddy,[a] Bobby Lee,[b] Steven G. Van Lanen,[b] Shannon Brown,[a]‡ Valérie de Crécy-Lagard,[c] Dirk Iwata-Reuyl[b] and Paul Schimmel[a]

[a]Departments of Chemistry and Molecular Biology, The Skaggs Institute for Chemical Biology, The Scripps Research Institute, BCC-379, La Jolla, CA 92037, USA, [b]Department of Chemistry, Portland State University, PO Box 751, Portland, OR 97207, USA, and [c]Department of Microbiology and Cell Science, University of Florida, PO Box 110700, Gainesville, FL 32611-0700, USA

‡ Current address: Department of Chemistry, Boston College, Chestnut Hill, MA 02467, USA.

Correspondence e-mail: swairjo@scripps.edu

Received 14 September 2005
Accepted 22 September 2005
Online 30 September 2005

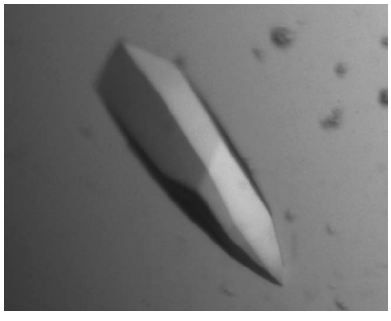

QueF (MW = 19.4 kDa) is a recently characterized nitrile oxidoreductase which catalyzes the NADPH-dependent reduction of 7-cyano-7-deazaguanine ($preQ_0$) to 7-aminomethyl-7-deazaguanine, a late step in the biosynthesis of the modified tRNA nucleoside queuosine. Initial crystals of homododecameric *Bacillus subtilis* QueF diffracted poorly to 8.0 Å. A three-dimensional model based on homology with the tunnel-fold enzyme GTP cyclohydrolase I suggested catalysis at intersubunit interfaces and a potential role for substrate binding in quaternary structure stabilization. Guided by this insight, a second crystal form was grown that was strictly dependent on the presence of $preQ_0$. This crystal form diffracted to 2.25 Å resolution.

1. Introduction

Prior to its use in translation, transfer RNA (tRNA) undergoes extensive post-transcriptional processing and maturation in all cells (for reviews, see Wolin & Matera, 1999; Hopper & Phizicky, 2003). Nucleoside modification is perhaps the most elaborate step in tRNA processing (Björk, 1995). Over 90 modified nucleosides have been characterized (McCloskey & Crain, 1998), many of which are conserved across broad phylogenetic boundaries (Grosjean *et al.*, 1995). Their modifications vary from simple methylation of the base or ribose ring to extensive hypermodification of the canonical bases, resulting in structural changes requiring multiple enzymatic steps. Here, we present the results of attempts to crystallize a complex protein assembly that is essential for synthesis of one of the most prevalent of these modifications.

Queuosine (Q) is a hypermodified guanosine found exclusively in the wobble position (position 34) of $tRNA_{GUN}$ coding for the amino acids asparagine, aspartate, histidine and tyrosine in eukarya and bacteria (Kersten & Kersten, 1990). The presence of Q in the anticodons of these tRNAs (including mitochondrial tRNAs) is compatible with a fundamental role in translation, specifically in modulating fidelity. For example, the −1 frameshifting events essential for correct translation of the retroviral Gag-Pol-Pro polypeptides of human T-cell lymphotropic virus and bovine leukemia virus appear to be dependent on (Q^-)-$tRNA^{Asn}$ (Jacks *et al.*, 1988; Hatfield *et al.*, 1989; Carlson *et al.*, 1999, 2000). Disruption of Q biosynthesis in the pathogenic bacterium *Shigella flexneri* results in loss of pathogenicity, making several enzymes in its biosynthesis pathway attractive targets for anti-shigellosis drugs. This loss is caused by mistranslation of *virF*, a transcription factor responsible for up-regulation of a suite of virulence-associated proteins (Durand *et al.*, 2000). Similarly, Q is essential in the biosynthesis of tyrosine in animals by its preventing a (Q^-)-tRNA-dependent mistranslation of mRNA coding for the tyrosine-biosynthesis enzyme phenylalanine hydroxylase (Marks & Farkas, 1997).

Q is characterized by a cyclopentenediol ring appended to 7-aminomethyl-7-deazaguanosine (Kasai *et al.*, 1975; Ohgi *et al.*, 1979). In some mammalian tRNAs, Q is glycosylated with galactose or mannose at the C5 hydroxyl (Okada & Nishimura, 1977). While Q

is acquired as a nutrient factor in eukarya, it is synthesized *de novo* in bacteria. Bacterial biosynthesis of Q starts with the conversion (by an unknown pathway) of GTP to 7-cyano-7-deazaguanine ($preQ_0$), followed by reduction to 7-aminomethyl-7-deazaguanine ($preQ_1$). $PreQ_1$ is then attached to tRNA by tRNA-guanine transglycosylase and further modified to Q in two *in situ* steps (Fig. 1). Using comparative genomics, QueF was identified as an enzyme family involved in Q biosynthesis (Reader *et al.*, 2004). QueF is an NADPH-dependent oxidoreductase that carries out the unprecedented reduction of a nitrile group ($preQ_0$) to a primary amine ($preQ_1$; Van Lanen *et al.*, 2005).

Based on their amino-acid sequences, QueF family members fall into two structural subfamilies (Van Lanen *et al.*, 2005). The YkvM subfamily is comprised of ∼160-amino-acid unimodular proteins with a characteristic QueF motif, *i.e.* E(S/L)K(S/A)*h*K(L/Y)(Y/F/W) (where *h* is a hydrophobic amino acid) bracketed on the N- and C-terminal sides by an invariant Cys and Glu, respectively. The YqcD subfamily of QueF enzymes is characterized by ∼280-amino-acid bimodular proteins in which the QueF motif and the invariant Cys and Glu are located separately in the weakly homologous N- and C-terminal halves (modules) of the polypeptide chain, respectively. Functional analysis of an enzyme from each subfamily, YkvM (*Bacillus subtilis* QueF) and YqcD (*E. coli* QueF), showed that YkvM enzymes function as homododecamers, while the YqcD enzymes are homodimers.

Homology between QueF and GTP cyclohydrolase I (GTP-CH-I) has been noted (Van Lanen *et al.*, 2005) and resulted in initial functional misannotation of the QueF gene family as GTP-CH-I in genomic databases. However, we used this homology to build a three-dimensional working model of *B. subtilis* QueF (19.4 kDa, 165 amino acids) based on the crystal structure of GTP-CH-I. The model allowed functional predictions that aided in understanding the crystallization properties of this YkvM subfamily member and enhanced the common prediction that the presence of substrate may improve crystal quality. The results and the general case of QueF discovery provide a powerful example of the use of bioinformatics tools to aid in proper functional assignment and consequent structural characterization of a new enzyme family.

2. Materials and methods

2.1. Three-dimensional homology modeling of *B. subtilis* QueF

A pairwise alignment of *B. subtilis* QueF and *E. coli* CTP-CH-I was extracted from a multiple sequence alignment of 30 QueF sequences and 30 GTP-CH-I sequences and used to build a three-dimensional model of a monomer of *B. subtilis* QueF in *MODELLER*-6 (v.1; John & Sali, 2003). The X-ray crystal structure of *Escherichia coli* GTP cyclohydrolase I (Nar *et al.*, 1995; GTP-CH-I; PDB code 1fbx) was used as a template. The *B. subtilis* QueF sequence was obtained from GenBank (accession No. NP_389258, GeneID 939296). The sequence similarity and identity between the two proteins is 26 and 14%, respectively. Using the symmetry of the GTP-CH-I decamer, a homodimer of the QueF monomeric model was generated. Using the coordinates of bound GTP in the GTP-CH-I structure, a 7-cyano-7-deazaguanine molecule was docked onto the putative active site that was located at the intersubunit interface. The final model was energy-minimized in *CNS* (Brünger *et al.*, 1998) and validated in *PROCHECK* (Vaguine *et al.*, 1999). The model had a standard Ramachandran plot with 90.2% of residues falling in favored regions and 8.3 and 1.5% in the allowed and generously allowed regions, respectively. The r.m.s. deviations of bonds and angles from standard values are 0.019 Å and 2.33°, respectively. A least-squares superposition with the GTP-CH-I structure yielded a good fit with an r.m.s. deviation of 0.64 Å over 318 C^{α} atoms.

2.2. Crystallization of *B. subtilis* QueF

N-terminal His_6-tagged *B. subtilis* QueF (GenBank NP_389258) was overexpressed, purified and processed for His_6-tag removal as described in Van Lanen *et al.* (2005). Prior to use in crystallization, the enzyme was dialyzed against 100 m*M* Tris pH 7.5, 100 m*M* KCl and 2 m*M* dithiothreitol. The substrate $preQ_0$ was synthesized as described previously (Van Lanen *et al.*, 2003).

B. subtilis QueF (15 mg ml^{-1}, apoenzyme) was subjected to high-throughput sparse-matrix and grid crystallization screens using the vapor-diffusion method. 200 nl sitting drops were set up using the Mosquito crystallization robot (Molecular Dimensions Ltd) in

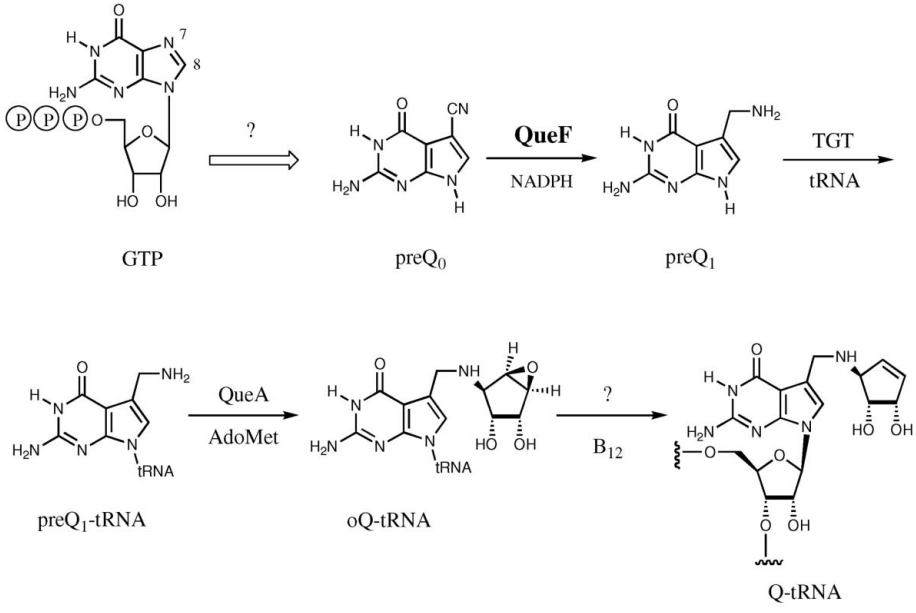

Figure 1
Biosynthetic pathway to queuosine in bacteria.

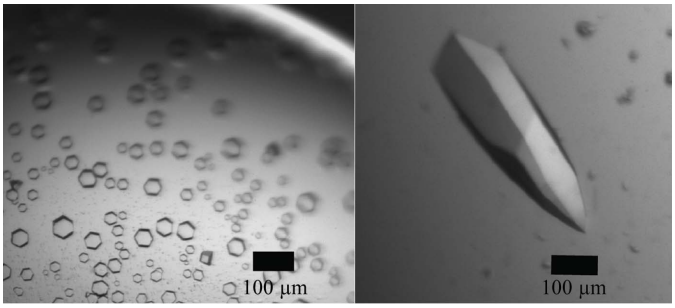

(*a*)

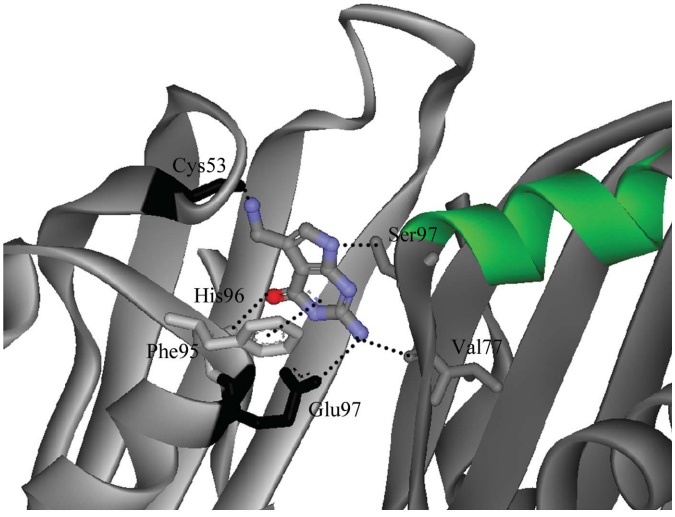

(*b*)

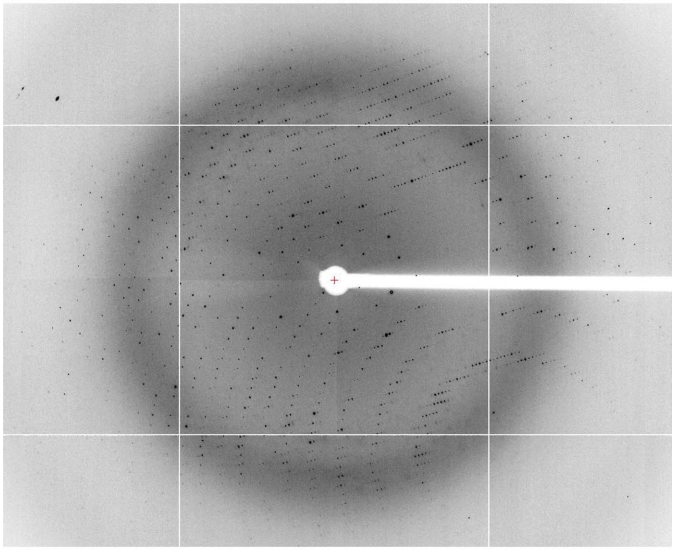

(*c*)

Figure 2
Crystals, three-dimensional model and X-ray diffraction of *B. subtilis* QueF. (*a*) Crystals of apoenzyme (hexagonal form, left) and of enzyme grown under the same conditions but pre-incubated with a sixfold excess of $preQ_0$ (trigonal form, right). (*b*) Putative active site of *B. subtilis* QueF based on the homology model built from the crystal structure of *E. coli* GTP-CH-I. The active site is located at the interface between two monomers shown in light and dark grey. The putative binding mode of the substrate's guanine is shown. Potential active-site interactions are indicated. The conserved QueF motif region is highlighted in green. The conserved Glu characteristic of T-fold enzymes and the invariant Cys shared between QueF and GTP-CH-I are shown in black. (*c*) A 0.5° oscillation image of the synchrotron X-ray diffraction of trigonal *B. subtilis* QueF. The image was taken at the SSRL beamline 1-5, with a 60 s exposure time. The crystal lasted 9 h in the beam before it denatured suddenly from radiation damage. The resolution at the edge of the detector was 2.15 Å.

Table 1
X-ray data-collection parameters.

Values in parentheses are for the highest resolution shell.

Wavelength (Å)	0.97944
Space group	$P3_121$
Unit-cell parameters (Å)	$a = b = 93.52$, $c = 193.76$
Crystal mosaicity (°)	0.29
Resolution range (Å)	2.25–50.0 (2.25–2.33)
No. of observations	278757 (17116)
No. of unique reflections	46429 (3890)
Completeness (%)	97.8 (83.3)
Redundancy	6.0 (4.3)
R_{merge}	0.078 (0.39)
$\langle I/\sigma(I)\rangle$	9.9 (7.9)
Matthews coefficient ($Å^3$ Da^{-1})	2.1
Solvent content (%)	40.1
Asymmetric unit content	6 monomers

96-well low-profile Greiner microplates (Greiner BioOne, FL, USA) and imaged with the CrystalPro imaging system (Tritek Corp., VA, USA). Crystallization experiments (1536) were performed at 293.15 and 277.15 K. Initial thick hexagonal plate crystals appeared in seven drops of various conditions. Crystals were reproduced manually at 293.15 K in hanging drops (1 µl) containing 4–15 mg ml^{-1} enzyme, 15–22%(*v*/*v*) polyethylene glycol 550 monomethyl ether (PEG 550 MME), 100 m*M* HEPES, Bis-Tris-propane or imidazole pH 7.2–7.8, 50 m*M* $CaCl_2$ and 0.05%(*w*/*v*) NaN_3 as a preservative. For crystallization in the presence of substrate, $preQ_0$ was dissolved in DMSO and directly added to the enzyme. The enzyme (4 mg ml^{-1}, ∼0.2 m*M*) was pre-incubated for 30 min on ice with 1.2–5 m*M* $preQ_0$ (enzyme: substrate molar ratio of 1:6–1:25). 1 µl sample was mixed with 1 µl reservoir solution containing 16–24%(*v*/*v*) PEG 550 MME, 100 m*M* HEPES or imidazole pH 7.2–7.8, 30 m*M* $CaCl_2$ and 0.05%(*w*/*v*) NaN_3. The mixed drop was equilibrated against 0.5 ml reservoir solution at 293.15 K until rod-shaped crystals grew in 2–3 weeks to a final size of 0.2 × 0.2 × 0.5 mm. Crystals were harvested and flash-cooled in liquid nitrogen without need for cryoprotection.

2.3. X-ray diffraction analysis

Crystals were screened for diffraction quality at beamline 11-1 of the Stanford Synchrotron Research Laboratory (SSRL), using a robot for mounting of crystals. A single-wavelength data set was collected from a crystal of the enzyme–$preQ_0$ complex on an ADSC Quantum 315 CCD detector at SSRL beamline 1-5 (crystal-to-detector distance 240 mm). Data were processed using the *HKL* package (Otwinowski & Minor, 1997).

3. Results

All attempts to crystallize the apoenzyme led to showers of single or clustered hexagonal crystal plates (0.05 × 0.1 × 0.1 mm, space group $P6_1$, unit-cell parameters $a = b = 81.6$, $c = 200.0$ Å) that grew from 15 mg ml^{-1} enzyme using PEG 3350, PEG 2000, PEG 1000 or PEG 550 MME as the precipitant, a variety of buffers in the pH range 6.0–9.0 and 50 m*M* $CaCl_2$. After refinement of conditions, the showering and clustering effects were controlled by lowering the $CaCl_2$ and protein concentrations to 30 m*M* and 4 mg ml^{-1}, respectively (Fig. 2*a*, left). However, the crystals remained highly mosaic (2.0–3.0°) and their diffraction quality poor as assessed by a lack of detectable diffraction beyond 7–8 Å resolution (data not shown). Previously reported crystals of *B. subtilis* YkvM (Midwest Center for Structural Genomics, ID APC35752) also diffracted poorly and were not pursued for structure determination (Anderson, 2005).

The similarity between *B. subtilis* QueF and GTP-CH-I in sequence and multimeric quaternary structure prompted us to predict a similar location for the active site of *B. subtilis* QueF, *i.e.* at the intersubunit interface. Based on the crystal structure of *E. coli* GTP-CH-I, a three-dimensional homology model of two adjacent QueF monomers was built and a $preQ_0$ molecule was docked in the putative active site (Fig. 2*b*). In one monomer, the docked substrate interacts with the two invariant side chains of Glu97 and Cys55 (two interactions also found in the structure of the GTP-CH-I–GTP complex; residue numbers are those of *B. subtilis* YkvM), the conserved Phe95 and the backbone NH of His96. In the other monomer, the side chain of Ser97 and the backbone CO of Val77 interact with substrate. Significantly, the QueF motif lies in a nearby α-helix. This model suggests that $preQ_0$ plays an important role in stabilizing and tying together the functional multimeric enzyme structure, bridging the two halves of the active site; that is, the QueF motif from one monomer and the invariant Glu and Cys from the other. This observation prompted us to test the effect of $preQ_0$ on the crystallization properties of QueF.

We used the refined conditions for crystal growth obtained for the apoenzyme [4 mg ml^{-1} protein, 20%(*v*/*v*) PEG 550 MME, 100 m*M* HEPES, 30 m*M* $CaCl_2$] and applied them to samples containing enzyme pre-incubated with $preQ_0$ (concentrations of 0.2, 0.4, 0.6, 0.8, 1.0, 1.2, 2 and 5 m*M*, *i.e.* enzyme:$preQ_0$ molar ratio of 1:1–1:25). To rule out the effect of DMSO, control experiments were set up simultaneously using enzyme pre-incubated with the same added volume of DMSO. A second trigonal crystal form (space group $P3_121$) appeared as the sole form only in drops containing $\geq$1.2 m*M* $preQ_0$ (enzyme:$preQ_0$ molar ratio $\geq$ 1:6, Fig. 2*a*, right). $PreQ_0$ concentrations of $\leq$ 0.8 m*M* (molar ratio $\leq$ 1:4) yielded the hexagonal form and intermediate concentrations yielded a mixture of both forms in the same drop. The trigonal form diffracted synchrotron X-rays to 2.25 Å with an apparent mosaicity of 0.29°. Analysis of the solvent content with the *CCP*4 package (Collaborative Computational Project, Number 4, 1994) gave a unique solution consisting of half a dodecamer in the asymmetric unit (Fig. 2*c*; Table 1). Growth of larger crystals was aided by inclusion of 1%(*w*/*v*) dextran sulfate or 100 m*M* imidazole in the crystallization buffer. Pre-incubation of enzyme with DMSO alone or with the cofactor for catalysis NADPH failed to produce the trigonal crystals (data not shown). A self-rotation search in *CNS* detected sixfold non-crystallographic symmetry around an axis parallel to the *c* axis of the unit cell. Because their unit-cell parameters differ significantly, it is unlikely that the two crystal forms are related. It is well known that use of substrates or substrate analogs in the crystallization process increases the chances of obtaining crystals or improving crystal quality. A dodecameric member of the tunnel-fold structural superfamily, the QueF quaternary arrangement is predicted to be a dimer of hexamers. Binding of substrate at the intersubunit interfaces may shift a hexamer–dodecamer equilibrium toward the dodecameric form, increasing sample homogeneity and allowing crystal growth around the twofold axis of the dodecamer as in the trigonal form. Although structure determination may be performed by molecular replacement, crystals of the selenomethionine-labeled protein have been produced and await collection of seleno-multiwavelength anomalous diffraction X-ray data.

We thank Drs Clyde Smith and Aina Cohen at SSRL beamlines 11-1 and 1-5, respectively, for help in X-ray data collection. The SSRL Structural Molecular Biology Program is supported by the Department of Energy, National Institutes of Health (NIH) and the National Institute of General Medical Sciences. This work was supported by grant No. GM15539 from the NIH and by a fellowship from the National Foundation for Cancer Research.

References

Anderson, W. (2005). Personal communication.
Björk, G. R. (1995). *tRNA: Structure, Biosynthesis and Function*, edited by U. L. RajBhandary, pp. 165–206. Washington DC: ASM Press.
Brünger, A. T., Adams, P. D., Clore, G. M., DeLano, W. L., Gros, P., Grosse-Kunstleve, R. W., Jiang, J.-S., Kuszewski, J., Nilges, M., Pannu, N. S., Read, R. J., Rice, L. M., Simonson, T. & Warren, G. L. (1998). *Acta Cryst.* D**54**, 905–921.
Carlson, B. A., Kwon, S. Y., Chamorro, M., Oroszlan, S., Hatfield, D. L. & Lee, B. J. (1999). *Virology*, **255**, 2–8.
Carlson, B. A., Kwon, S. Y., Lee, B. J. & Hatfield, D. (2000). *Mol. Cell*, **10**, 113–118.
Collaborative Computational Project, Number 4 (1994). *Acta Cryst.* D**50**, 760–763.
Durand, J. M., Dagberg, B., Uhlin, B. E. & Björk, G. R. (2000). *Mol. Microbiol.* **35**, 924–935.
Grosjean, H., Sprinzl, M. & Steinberg, S. (1995). *Biochimie*, **77**, 139–141.
Hatfield, D., Feng, Y.-X., Lee, B. J., Rein, A., Levin, J. G. & Oroszlan, S. (1989). *Virology*, **173**, 736–742.
Hopper, A. K. & Phizicky, E. M. (2003). *Genes Dev.* **17**, 162–180.
Jacks, T., Madhani, H. D., Masiarz, F. R. & Varmus, H. F. (1988). *Cell*, **55**, 447–458.
John, B. & Sali, A. (2003). *Nucleic Acids Res.* **31**, 3982–3992.
Kasai, H., Ohashi, Z., Harada, F., Nishimura, S., Oppenheimer, N. J., Crain, P. F., Liehr, J. G., von Minden, D. L. & McCloskey, J. A. (1975). *Biochemistry*, **14**, 4198–4208.
Kersten, H. & Kersten, W. (1990). *Chromatography and Modification of Nucleosides Part B*, edited by K. C. T. Kuo, pp. B69–B108. Amsterdam: Elsevier.
McCloskey, J. A. & Crain, P. F. (1998). *Nucleic Acids Res.* **26**, 196–197.
Marks, T. & Farkas, W. R. (1997). *Biochem. Biophys. Res. Commun.* **230**, 233–237.
Nar, H., Huber, R., Meining, W., Schmid, C., Weinkauf, S. & Bacher, A. (1995). *Structure*, **3**, 459–466.
Ohgi, T., Kondo, T. & Goto, T. (1979). *J. Am. Chem. Soc.* **101**, 3629–3633.
Okada, N. & Nishimura, S. (1977). *Nucleic Acids Res.* **4**, 2931–2937.
Otwinowski, Z. & Minor, W. (1997). *Methods Enzymol.* **276**, 307–326.
Reader, J., Metzgar, D., Schimmel, P. & de Crécy-Lagard, V. (2004). *J. Biol. Chem.* **279**, 6280–6285.
Vaguine, A. A., Richelle, J. & Wodak, S. J. (1999). *Acta Cryst.* D**55**, 191–205.
Van Lanen, S. G., Kinzie, S. D., Matthieu, S., Link, T., Culp, J. & Iwata-Reuyl, D. (2003). *J. Biol. Chem.* **278**, 10491–10499.
Van Lanen, S. G., Reader, J. S., Swairjo, M. A., de Crécy-Lagard, V., Lee, B. & Iwata-Reuyl, D. (2005). *Proc. Natl Acad. Sci. USA*, **102**, 4264–4269.
Wolin, S. L. & Matera, A. G. (1999). *Genes Dev.* **13**, 1–10.